^{31}P and ^{183}W NMR Spectroscopic Evidence for Novel Peroxo Species in the "$H_3[PW_{12}O_{40}]\cdot yH_2O/H_2O_2$" System. Synthesis and X-ray Structure of Tetrabutylammonium (μ-Hydrogen phosphato)bis(μ-peroxo)bis(oxoperoxotungstate)(2−): A Catalyst of Olefin Epoxidation in a Biphase Medium

Laurent Salles,† Catherine Aubry,† René Thouvenot,*,‡ Françis Robert,‡ Claudine Dorémieux-Morin,† Geneviève Chottard,‡ Henry Ledon,§ Yves Jeannin,‡ and Jean-Marie Brégeault*,†

URA 1428, Catalyse et Chimie des Surfaces, and URA 419, Chimie des Métaux de Transition, Département de Chimie, Université Pierre et Marie Curie, Case 196, Tour 54–55, 4 Place Jussieu, 75252 Paris Cedex 05, France, and Chemoxal/L'Air Liquide, 75 Quai d'Orsay, 75321 Paris Cedex 07, France

Received May 28, 1993⊗

Both the "$H_3[PW_{12}O_{40}]\cdot yH_2O$" and the "$H_2WO_4/H_2O_2$–$H_2O/H_3PO_4$" systems show several ^{31}P and ^{183}W NMR signals which may be assigned to new phosphatooxoperoxotungstate species, $[PW_xO_y]^{\omega-}$, (x = 1–4). Among these complexes, the novel "PW_2" anion was studied in the crystalline state and in solution. Several salts of the general formula $Q_2[HPO_4\{WO(O_2)_2\}_2]$ were obtained by the reaction of tungstic acid, "H_2WO_4", or $H_3[PW_{12}O_{40}]\cdot yH_2O$ with hydrogen peroxide, orthophosphoric acid, and the appropriate onium salt, QX ($Q^+ = [(n\text{-}C_4H_9)_4N]^+$; $[\{(C_6H_5)_3P\}_2N]^+$; $[\{(C_{18}H_{37})\,75\% + (C_{16}H_{33})\,25\%\}_2N(CH_3)_2]^+$). The structure of $[(n\text{-}C_4H_9)_4N]_2[HPO_4\{WO(O_2)_2\}_2]$ (triclinic $P\bar{1}$, a = 10.660(3) Å, b = 12.662(3) Å, c = 17.723(3) Å, α = 74.92(2)°, β = 77.57(2)°, γ = 86.65(2)°, Z = 2) was refined to R = 0.060 and R_w = 0.065. The polyanion has one nonbridging and one bridging peroxo group on each W center with slightly elongated peroxo bonds (1.53(3) and 1.56(4) Å) in the former case. The structural features compare well with those of previously described complexes, $[(n\text{-}C_6H_{13})_4N]_3[PM_4O_{24}]$ (M = Mo or W). The vibrational (IR and Raman) and ^{31}P with ^{183}W NMR spectra suggest that the overall structure is maintained in organic solvents at room temperature. (R)-(+)-Limonene is stoichiometrically epoxidized at this temperature. The two tungsten(VI) compounds $[(n\text{-}C_4H_9)_4N]_2[HPO_4\{WO(O_2)_2\}_2]$ and $[(n\text{-}C_4H_9)_4N]_3[PW_4O_{24}]$, are about 30 times more active than $[(n\text{-}C_4H_9)_4N]_3[PMo_4O_{24}]$. These differences can be related to the observed ν(O–O) frequencies (IR and Raman, both solid-state and solution spectra).

Introduction

Selective epoxidation of olefins has been extensively studied and is still a subject of interest.[1–5]

While studying oxidation reactions in a biphase medium and/or by phase transfer catalysis (PTC), we became interested in comparing anionic peroxo complexes formed either from hydrogen peroxide and heteropolyacids,[2] HPA, $H_n[XM_{12}O_{40}]\cdot yH_2O$ (X = P, Si; M = Mo, W), or from H_2O_2 and tungstic acid, "H_2WO_4", in the presence of orthophosphoric acid.[3] It has been shown that the Venturello complex, $Q_3[PO_4\{WO(O_2)_2\}_4]$ (**1**) where Q^+ is a quaternary ammonium ion, can be prepared by employing Ishii's method involving HPA and H_2O_2.[4] More recently, several salts of the general formula $Q_3[PMo_4O_{24}]$ (**2**) were obtained by the reaction of molybdenum trioxide, MoO_3, or $Na_2H[PMo_{12}O_{40}]\cdot yH_2O$ with hydrogen peroxide, H_3PO_4, and the appropriate onium salt.[5] We showed that the $[PMo_4O_{24}]^{3-}$ anion is identical with the species described by a Russian group in the "$H_2MoO_4/H_2O_2/H_3PO_4$/2-aminopyridine" system.[6] IR and Raman spectroscopy and ^{31}P NMR (analysis of the tungsten satellite subspectra with $Q_3[PW_4O_{24}]$) show that $[PM_4O_{24}]^{3-}$ anions are stable in solution and that the overall structure is conserved in aqueous as well as in organic solvents ($CHCl_3$, $C_2H_4Cl_2$, MeCN, etc.). Both the "$H_3[PW_{12}O_{40}]\cdot yH_2O/H_2O_2/H_3PO_4$" and the "$H_2WO_4/H_2O_2/H_3PO_4$" systems show several ^{31}P NMR signals which can be assigned to new *phosphatooxoperoxotungstate* species, $[PW_xO_y]^{\omega-}$.

^{183}W NMR spectroscopy has been shown to be a powerful tool in polytungstate chemistry.[7–9] We have applied ^{31}P and ^{183}W

---

† URA 1428.

‡ URA 419.

§ Chemoxal/L'Air Liquide.

⊗ Abstract published in *Advance ACS Abstracts*, February 1, 1994.

(1) (a) Petrignani, J.-F. In *The Chemistry of the Metal-Carbon Bond*; Hartley, F. R., Ed.; Wiley: London, 1989; p 63 and references therein. (b) Mimoun, H. In *The Chemistry of Peroxide*; Patai, S., Ed.; Wiley: New York, 1983; p 465. (c) Sheldon, R. A. *Chemtech* 1991, 566. (d) Sheldon, R. A. In *Dioxygen Activation and Homogeneous Catalytic Oxidation*; Simandi, L. I., Ed.; Elsevier: Amsterdam, 1991; p 573. (e) Herrman, W. A.; Fischer, R. W.; Marz, D. W. *Angew. Chem., Int. Ed. Engl.* **1991**, *30*, 1638. (f) Brégeault, J.-M. *Catalyse Homogène par les Complexes des Métaux de Transition*; Masson: Paris, 1992; p 193.

(2) (a) Kuznetsova, L. I.; Maksimovskaya, R. I.; Fedotov, M. A.; Matveev, K. I. *Izv. Akad. Nauk. SSSR, Ser. Khim.* (*Engl. Transl.*) **1983**, 666. Kuznetsova, L. I.; Maksimovskaya, R. I.; Fedotov, M. A. *Izv. Akad. Nauk. SSSR, Ser. Khim.* (*Engl. Transl.*) **1985**, 488. (b) Ishii, Y.; Yamawaki, K.; Yoshida, T.; Ura, T.; Ogawa, M. *J. Org. Chem.* **1987**, *52*, 1868. Ishii, Y.; Yamawaki, K.; Ura, T.; Yamada, H.; Yoshida, T.; Ogawa, M. *J. Org. Chem.* **1988**, *53*, 3587. Sakaue, S.; Sakata, Y.; Nishiyama Y.; Ishii, Y. *Chem. Lett.* **1992**, 289.

(3) (a) Venturello, C.; D'Aloisio, R.; Bart, J. C. J.; Ricci, M. *J. Mol. Catal.* **1985**, *32*, 107. (b) Venturello, C.; D'Aloisio, R. *J. Org. Chem.* **1988**, *53*, 1553. Venturello, C.; Alneri, E.; Ricci, M. *J. Org. Chem.* **1983**, *48*, 3831. Venturello, C.; Gambaro, M. *Synthesis Commun.* **1989**, 295. Venturello, C.; D'Aloisio, R.; Ricci, M. Montedison Co., Eur. Pat. Appl. 0109 273, 1984. Venturello, C.; Gambaro, M. Montedison Co., Eur. Pat. Appl. 0146 374, 1985. Venturello, C.; Gambaro, M. *J. Org. Chem.* **1991**, *56*, 5924.

(4) (a) Brégeault, J.-M.; Aubry, C.; Chottard, G.; Platzer, N.; Chauveau, F.; Huet, C.; Ledon, H. In *Dioxygen Activation and Homogeneous Catalytic Oxidation*; Simandi, L. I., Ed.; Elsevier: Amsterdam, 1991; p 521. (b) Aubry, C.; Chottard, G.; Platzer, N.; Brégeault, J.-M.; Thouvenot, R.; Chauveau, F.; Huet, C.; Ledon, H. *Inorg. Chem.* **1991**, *30*, 4409.

(5) Salles, L.; Aubry, C.; Robert, F.; Chottard, G.; Thouvenot, R.; Ledon, H.; Brégeault, J.-M. *New J. Chem.* **1993**, *17*, 367.

(6) Beiles, R. G.; Rozmanova, Z. E.; Andreeva, O. B. *Russ. J. Inorg. Chem.* (*Engl. Transl.*) **1969**, *14*, 1122.

(7) Acerete, R.; Hammer, C. F.; Baker, L. C. W. *J. Am. Chem. Soc.* **1979**, *101*, 267. Acerete, R.; Hammer, C. F.; Baker, L. C. W. *J. Am. Chem. Soc.* **1982**, *104*, 5384. Acerete, R.; Hammer, C. F.; Baker, L. C. W. *Inorg. Chem.* **1984**, *23*, 1478. Jorris, T. L.; Kozik, M.; Casañ-Pastor, N.; Domaille, P. J.; Finke, R. G.; Miller, W. K.; Baker, L. C. W. *J. Am. Chem. Soc.* **1987**, *109*, 7402. Acerete, R.; Server-Carrio, J.; Vegas, A.; Martinez-Ripoll, M. *J. Am. Chem. Soc.* **1990**, *112*, 9386.

0020-1669/94/1333-0871$04.50/0

NMR spectroscopy to characterize the key species in *phosphatooxoperoxo complex* chemistry in aqueous solution. We have already demonstrated that some of the peroxo complexes formed from $H_3[PW_{12}O_{40}]\cdot yH_2O$ and various concentrations of hydrogen peroxide can be identified by ^{31}P and ^{183}W NMR.[4b] Our previous investigations were limited to the characterization of the $[PO_4\{WO(O_2)_2\}_4]^{3-}$ and the $[W_2O_3(O_2)_4(H_2O)_2]^{2-}$ anions which can be transferred to organic media (MeCN/$CDCl_3$ or pure $CDCl_3$) as onium salts.

Among the different complexes of the general formula $[PW_xO_y]^{\omega-}$, identified spectroscopically in aqueous solution, we were able to isolate the novel "PW_2" anion which is probably structurally related to the anion of the compound, $[(n\text{-}C_4H_9)_4N]_2[C_6H_5PO_3W_2O_{10}]$ (**3**) prepared from the "H_2WO_4/H_2O_2/$[(n\text{-}C_4H_9)_4N]_2[C_6H_5PO_3]$" system.[10] The structure of **3**, which is essential for the understanding of the catalytic activity, has not yet been established. We wish to report here an investigation of several "PW_2" complexes in the crystalline state and in solution. We present the crystal structure of $[(n\text{-}Bu)_4N]_2[HPW_2O_{14}]$ (**4a**); these crystal data are compared with those of other well-documented bi- and polynuclear peroxotungsten species with different kinds of bridging ligands. In order to obtain information on the μ-hydrogen phosphato group, high-resolution ^1H NMR spectra of **4a** are analyzed. Vibrational spectroscopy together with ^{31}P and ^{183}W NMR has been used to study the nature of solute species in solution of **4a**, and we have conducted a brief survey on the epoxidizing ability of such solutions compared with those obtained from $[PM_4O_{24}]^{3-}$ (M = Mo or W). The catalytic properties of $Q_2[HPW_2O_{14}]$ in a biphase medium are also presented (epoxidation of (*R*)-(+)-limonene).

Experimental Section

Materials. $H_3[PW_{12}O_{40}]\cdot yH_2O$, $H_4[SiW_{12}O_{40}]\cdot yH_2O$, and tungstic acid, "$H_2WO_4$", were hydrated commercial products (Janssen, Fluka, and Eurotungstène, respectively) used without further purification. The 30% aqueous solutions of hydrogen peroxide were purchased from Prolabo (phosphorus concentration between 12.5 and 19.2 mM) for syntheses and from Aldrich (phosphorus concentration lower than 1.6 mM) for NMR experiments and catalytic tests. (*R*)-(+)-Limonene (Aldrich) was better than 97% pure by GC analysis. The onium salts, $[(n\text{-}C_4H_9)_4N]Cl$ and $[\{(C_6H_5)_3P\}_2N]Cl$, denoted as (PPN)Cl, were purchased from Aldrich. The phase transfer agent was a mixture of two quaternary ammonium chlorides, $[\{(C_{18}H_{37})\ 75\% + (C_{16}H_{33})\ 25\%\}_2N(CH_3)_2]Cl$, marketed by Akzo under the name of Arquad 2HT. It was used after being washed several times with acetone, followed by air drying.

Spectroscopic Techniques. The ^{31}P NMR spectra were recorded in 10-mm-o.d. tubes (passivated by treatment with a surfactant or with 10% HNO_3/10% H_2O_2) on a Bruker WM 250, AM 500, or MSL 400 apparatus operating at 101.2, 202.4, or 162 MHz, respectively, in the Fourier transform mode. ^{183}W NMR spectra were recorded on a AM 500 or MSL 400 apparatus equipped with a broad-band VSP probehead, at 20.8 or 16.6 MHz, respectively. Generally, tungsten NMR spectra were obtained immediately after phosphorus spectra, on the same solutions, by simply retuning the probehead. Control experiments show that tungsten and phosphorus spectra are related to the same solution species. ^{183}W chemical shifts were measured with respect to an external 2M Na_2WO_4 solution in alkaline D_2O by using saturated tetrahydrogen silicododecatungstate ($H_4[SiW_{12}O_{40}\cdot yH_2O]$) in D_2O as a secondary standard (δ = −103.8 ppm), and ^{31}P chemical shifts were referenced with respect to external 85% H_3PO_4. The chemical shifts were not corrected for bulk magnetic susceptibility. The aqueous solutions for the ^{31}P and ^{183}W NMR studies were obtained by dissolving trihydrogen phosphododecatungstate, $H_3[PW_{12}O_{40}]\cdot yH_2O$, in water; then the desired amounts of 30% aqueous hydrogen peroxide and finally of 6 M aqueous phosphoric acid were added with stirring. The colorless solutions were then transferred directly into the NMR tubes, and 10% D_2O was added (c_w = 1 M). The spectra presented in Figures 1 and 2 are typical of the $H_3[PW_{12}O_{40}]$/H_2O_2 system with a high $[H_2O_2]/[W]$ ratio; these solutions did not evolve over a period of 1 week. For the quantitative determination of the stoichiometry of the "PW_n" species in the aqueous solution, a 5-mm-o.d. tube containing authentic $H_3[PW_{12}O_{40}]\cdot yH_2O$ was placed concentrically in the 10-mm NMR tube.

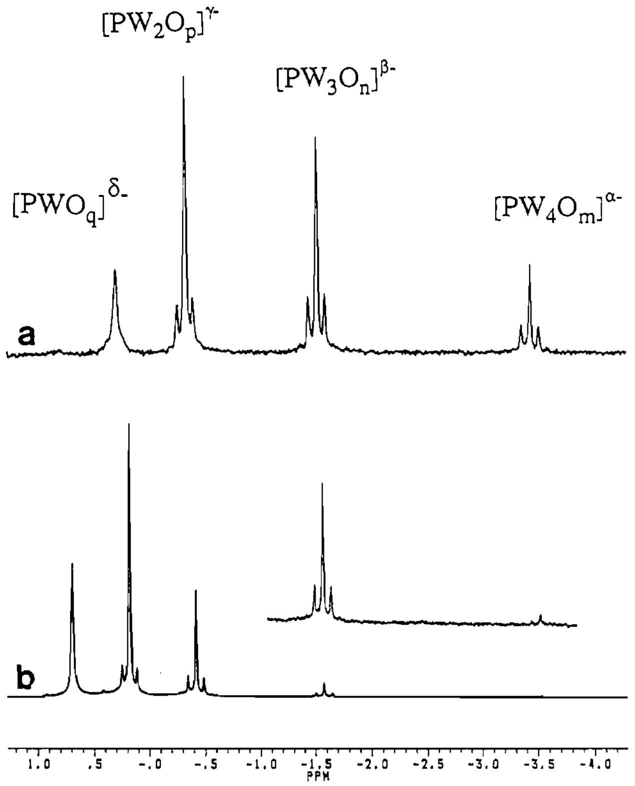

Figure 1. 162 MHz ^{31}P NMR spectra of the $[PW_xO_y]^{\omega-}$ anions: (a) "$H_3[PW_{12}O_{40}]\cdot yH_2O/H_2O_2$" system, $[H_2O_2]/[W] \approx 7{:}1$ (320 scans); (b) same as part a with added H_3PO_4, $[H_2O_2]/[W]/[H_3PO_4] \approx 7{:}1{:}0.75$ (768 scans).

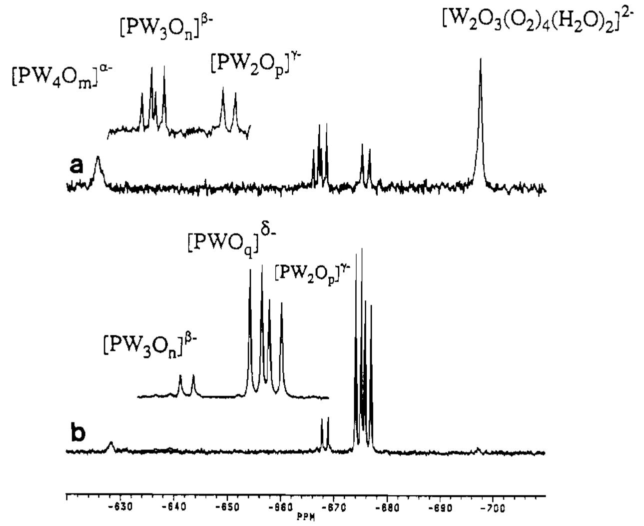

Figure 2. 16.6-MHz ^{183}W NMR spectra of the $[PW_xO_y]^{\omega-}$ anions and of oxoperoxotungstates: (a) "$H_3[PW_{12}O_{40}]\cdot yH_2O/H_2O_2$" system, $[H_2O_2]/[W] \approx 7{:}1$ (17776 scans); (b) same as part a with added H_3PO_4, $[H_2O_2]/[W]/[H_3PO_4] \approx 7{:}1{:}0.75$ (60 888 scans).

---

(8) (a) Minelli, M.; Enemark, J. M.; Browlee, R. T. C.; O'Connor, M. J.; Wedd, A. G. *Coord. Chem. Rev.* **1985**, *68*, 244 and references therein. (b) Lefebvre, J.; Chauveau, F.; Doppelt, P.; Brevard, C. *J. Am. Chem. Soc.* **1981**, *103*, 4589. (c) Jeannin, Y.; Martin-Frère, J. *J. Am. Chem. Soc.* **1981**, *103*, 1664. (d) Domaille, P. J.; Knoth, W. H. *Inorg. Chem.* **1983**, *22*, 818. (e) Domaille, P. J. *J. Am. Chem. Soc.* **1984**, *106*, 7677. (f) Brévard, C.; Schimpf, R.; Tourné, G. F.; Tourné, C. M. *J. Am. Chem. Soc.* **1983**, *105*, 7059. (g) Finke, R. G.: Droege, M. W. *Inorg. Chem.* **1983**, *22*, 1006. (h) Finke, R. G.; Rapko, B.; Saxton, R. J.; Domaille, P. J. *J. Am. Chem. Soc.* **1986**, *108*, 2947; (i) Tourné, C. M.; Tourné, G. F.; Zonnevijlle, F. *J. Chem. Soc., Dalton Trans.* **1991**, 143.

(9) Canny, J.; Thouvenot, R.; Tézé, A.; Hervé, G.; Leparulo-Loftus, M.; Pope, M. T. *Inorg. Chem.* **1991**, *30*, 976.

(10) Quenard, M. Thesis, Université Claude Bernard, Lyon, France, 1985. Quenard, M.; Bonmarin, V.; Gelbard, G.; Krumenacker, L. *New J. Chem.* **1989**, *13*, 183.

Table 1. Crystallographic Data for Compound $(n\text{-}Bu_4N)_2[HPW_2O_{14}]$ (**4a**)

chem formula: $C_{32}H_{73}N_2O_{14}PW_2$
a = 10.660(3) Å
b = 12.662(3) Å
c = 17.723(3) Å
α = 74.92(2)°
β = 77.57(2)°
γ = 86.65(2)°
V = 2255(15) Å^3
Z = 2

fw = 1108.61
space group: $P\bar{1}$ (No. 2)
T = 20 °C
λ = 0.710 69 Å
ρ_{obsd} = 1.61 g cm^{-3}
ρ_{calcd} = 1.63 g cm^{-3}
μ = 52.97 cm^{-1}
R^a = 0.0597
$R_w{}^b$ = 0.0654

[a] $R = \sum(||F_o| - |F_c||)/\sum|F_o|$. [b] $R_w = [\sum w(||F_o| - |F_c||)^2/\sum w|F_o|^2]^{1/2}$.

The ^1H high-resolution NMR spectrum of $(n\text{-}Bu_4N)_2[HPW_2O_{14}]$, in the solid state, was recorded at room temperature on a Bruker MSL 400 apparatus at 400 MHz. The sample was contained in a thin 6-mm-o.d. sealed glass tube. After recording the MAS spectrum (3000 Hz), the MAS + echo method recommended by Olejniczak[11] was used, the time between echo pulses being equal to the sample spinning period (MAS frequency 2870 Hz). Under such conditions, the areas under the signals are no longer proportional to the number of spins, because the method favors species which are immobile in the lattice during the rotation period. The isotropic values of the chemical shift are expressed with the usual conventions, without magnetic susceptibility corrections.

Raman spectra were recorded on a Jobin-Yvon U_{1000} spectrometer with a resolution of 4 cm^{-1}. The 514.5-nm exciting line of an Ar^+ laser was used at 80–100 mW. Solid samples of the tungsten complex were mounted on a disk rotating at about 1000 rpm in order to avoid decomposition and/or photoreduction by the laser beam.

IR spectra were measured on a Fourier transform apparatus (Bruker IFS 45) with solid samples in Nujol suspension between two cesium bromide plates. Solution spectra of **4a** (0.1 mM) were recorded with a standard sodium chloride cell (0.1 mm thickness). Acetonitrile has a window at 650–910 cm^{-1} which is suitable for studying ν(O–O) bands.

X-ray Crystallography. Since compound **4a** is air-stable, no special care was taken when mounting the crystal. Diffraction data were collected on an Enraf-Nonius CAD-4 automated diffractometer at room temperature, using Mo Kα graphite-monochromated radiation (λ = 0.710 69 Å). Accurate unit cell parameters were obtained from least-squares refinement of 25 reflections in the 14–15° θ range. The intensities of two standard reflections measured every hour showed no significant variations. Intensity data were collected in the $\theta/2\theta$ scan mode for $2.0 < 2\theta < 50°$. The intensities were corrected for Lorentz and polarization factors as well as for absorption using DIFABS.[12] Due to the small crystal size, of the 7895 independent reflections measured, 2931 with $(I) \geq 3\sigma(I)$ were used for the structure determination and refinement. Table 1 lists crystallographic data for compound **4a**.

The two tungsten atoms were located on a Patterson map and all other atoms were found in subsequent Fourier maps. Least-squares refinement was carried out in three blocks (462 parameters) with anisotropic thermal parameters for all non-hydrogen atoms. Hydrogen atoms were not located. The function minimized was $\sum w(|F_o| - |F_c|)^2$ (w = 1.0). The real and imaginary parts of the form factors for all atoms were taken from ref 13. Calculations were performed using CRYSTALS.[14] The final difference Fourier map showed residual maxima and minima of 1.7 and 1.4 e Å^{-3} near the tungsten atoms. Final values of the positional parameters for all non-hydrogen atoms are given in Table 2.

Stoichiometric Oxidation Reactions with $Q_3[PM_4O_{24}]$ and with $Q_2[HPW_2O_{14}]$, Q^+ = $(n\text{-}Bu_4N)^+$. These were conducted under nitrogen using Schlenk techniques and deaerated solvents. To a thermostated (20 °C) solution of the complex (O_{peroxo}: 1 mmol) in 5 mL of dry CH_2Cl_2 was rapidly added 1.5 mmol of (*R*)-(+)-limonene (**5**). The solution was stirred under pure nitrogen. GC analysis was performed with *n*-decane as internal standard.

Catalytic Tests. Experimental Procedure. First 30% hydrogen peroxide (1 mL; 9.8 mmol) was added to the W(VI)-based precursor along with 2 mL of water. After 15 min of stirring (necessary for the precursor to react completely), the solution was transferred to a Schlenk tube containing a $CHCl_3$ solution of Arquad 2HT (5 mL, 8.5 mM). At this stage, ^{31}P NMR showed that $[HPW_2O_{14}]^{2-}$ was present in the organic phase (see Syntheses of Peroxo Complexes (c)). After the two phases had been stirred for 2 min, (*R*)-(+)-limonene (6.2 mmol) was added. The mixture was then stirred at room temperature. GC analysis was usually performed directly on the organic phase.

Table 2. Fractional Atomic Coordinates and Estimated Standard Deviations

atom	*x/a*	*y/b*	*z/c*	*U*(eqv), Å^2
W(1)	–0.1548(1)	–0.02302(9)	0.29940(7)	0.0715
W(2)	–0.0711(1)	0.25017(9)	0.19800(7)	0.0779
P(1)	–0.0515(9)	0.0532(6)	0.1051(5)	0.0847
O(1)	–0.129(2)	–0.016(2)	0.188(1)	0.1075
O(2)	–0.097(2)	–0.145(1)	0.324(1)	0.1001
O(3)	–0.334(2)	–0.068(2)	0.313(2)	0.1143
O(4)	–0.302(2)	–0.037(2)	0.384(1)	0.1171
O(5)	–0.089(2)	0.056(1)	0.357(1)	0.0962
O(6)	–0.015(2)	0.079(1)	0.271(1)	0.0785
O(7)	–0.021(2)	0.161(1)	0.123(1)	0.0931
O(8)	–0.123(2)	0.365(1)	0.138(1)	0.1030
O(9)	0.101(3)	0.295(2)	0.192(2)	0.0864
O(10)	–0.019(4)	0.319(2)	0.253(2)	0.1584
O(11)	–0.209(2)	0.229(2)	0.291(1)	0.1298
O(12)	–0.218(2)	0.154(1)	0.242(1)	0.0940
O(13)	0.073(2)	–0.007(2)	0.082(1)	0.1026
O(14)	–0.125(2)	0.072(2)	0.041(1)	0.0958
N(1)	–0.323(2)	–0.122(2)	0.651(1)	0.0819
C(1)	–0.370(2)	–0.026(2)	0.587(2)	0.0734
C(2)	–0.282(3)	0.074(3)	0.555(2)	0.1143
C(3)	–0.359(4)	0.148(3)	0.498(2)	0.1404
C(4)	–0.327(6)	0.263(3)	0.480(3)	0.2102
C(5)	–0.189(3)	–0.161(2)	0.614(2)	0.0912
C(6)	–0.191(3)	–0.217(3)	0.547(2)	0.1279
C(7)	–0.046(4)	–0.248(3)	0.517(3)	0.1457
C(8)	–0.045(5)	–0.370(4)	0.541(5)	0.2421
C(9)	–0.426(3)	–0.211(3)	0.675(2)	0.0841
C(10)	–0.402(4)	–0.311(3)	0.737(2)	0.1326
C(11)	–0.509(4)	–0.399(4)	0.729(3)	0.1726
C(12)	–0.499(6)	–0.499(5)	0.795(3)	0.2792
C(13)	–0.292(3)	–0.081(3)	0.720(2)	0.1193
C(14)	–0.421(5)	–0.042(4)	0.770(3)	0.1717
C(15)	–0.37(1)	–0.015(6)	0.840(3)	0.2109
C(16)	–0.47(1)	0.035(9)	0.883(4)	0.3367
N(2)	0.012(2)	0.354(2)	–0.167(1)	0.0852
C(21)	0.096(3)	0.270(2)	–0.111(2)	0.1031
C(22)	0.173(4)	0.328(3)	–0.074(2)	0.1321
C(23)	0.272(4)	0.230(4)	–0.045(3)	0.1709
C(24)	0.345(6)	0.281(5)	0.001(4)	0.2715
C(25)	–0.058(4)	0.279(3)	–0.199(3)	0.1159
C(26)	–0.131(5)	0.353(5)	–0.257(4)	0.1569
C(27)	–0.204(8)	0.278(8)	–0.264(5)	0.2604
C(28)	–0.288(9)	0.331(8)	–0.330(5)	0.2746
C(29)	–0.076(4)	0.428(3)	–0.121(2)	0.1134
C(30)	–0.177(4)	0.357(4)	–0.054(2)	0.1258
C(31)	–0.261(6)	0.457(6)	–0.035(3)	0.2350
C(32)	–0.347(6)	0.369(6)	0.027(4)	0.2508
C(33)	0.096(3)	0.432(2)	–0.236(2)	0.1010
C(34)	0.202(3)	0.375(3)	–0.290(2)	0.1281
C(35)	0.257(5)	0.460(4)	–0.365(3)	0.1490
C(36)	0.354(5)	0.409(5)	–0.418(3)	0.1688

Analysis and Identification of Products. GC/MS Data System. All reaction mixtures were analyzed on a Delsi 30 gas chromatograph equipped with a 0.25 mm × 50 m OV 1701 capillary column and a flame ionization detector linked to a Delsi Enica 10 electronic integrator (**6a** and **6b** give well-resolved peaks). Product yields were determined by using straight-chain hydrocarbons as internal standards. Detector response factors were calibrated by using stock solutions of authentic samples at concentrations similar to those encountered in the oxidation reactions. Cumulative errors resulting from response factor calibration, base line treatment, purity of standards, etc. are believed to be 5–8% or less in most cases.

Mass spectral data were obtained at 70 eV on a mass spectrometer (Delsi-Nermag) coupled with a GC apparatus (Girdel 30). (+)-Limonene oxide (mixture of *cis* and *trans*) was obtained in 55% yield and was identified by MS. **6a**: *m/z* 137 (5.7%), 119 (2.7), 109 (9.5), 108 (8.1), 94 (2.7), 93 (5.9), 79 (14.9), 67 (8.0), 53 (5.4), 43 (100). **6b**: *m/z* 137

---

(11) Olejniczak, E. T.; Vega, S.; Griffin, R. G., *J. Chem. Phys.* **1984**, *81*, 4804.

(12) Walker, N.; Stuart, D. *Acta Crystallogr.* **1983**, *139*, 158.

(13) Cromer, D. T.; Waber, J. T. *International Tables for X-ray Crystallography*, Kynoch Press: Birmingham, 1974; Vol. IV, p 99.

(14) Watkins, D. T.; Carruthers, J. R.; Betteridge, P. W. *CRYSTALS User Guide*; Chemical Crystallography Laboratory, University of Oxford: Oxford, 1985.

(0.8%), 119 (0.5), 109 (4.5), 108 (13.0), 94 (13.5), 93 (5.4), 79 (10.8), 67 (8.1), 53 (6.7), 43 (100). The mixture of *cis* and *trans* limonene oxides was isolated by preparative GC (20% SE 30 on Chromosorb W at 50 °C) and identified by ^1H and ^{13}C NMR. **6a** and **6b** gave only well-resolved signals at 3 and 4.7 ppm. ^1H NMR (ppm): **6a**, $\delta = 2.99$ (d, $J = 5.2$ Hz, H-2), 4.66 (m, $=CH_2$); **6b**, $\delta = 3.05$ (t, $J = 2.1$ Hz, H-2), 4.72 (m, $=CH_2$). ^{13}C NMR (ppm): (**6a** + **6b**), $\delta = 149.1$ (C_8), 108.9 (C_9), 59.1 (C_1), 57.4 (C_2), 40.6 (C_4), 21.0 (C_{10}).

Syntheses of Peroxo Complexes from "$H_2WO_4/H_2O_2/H_3PO_4$". Preparation of $Q_2[HPO_4\{WO(O_2)_2\}_2]$ (4): (a) $Q^+ = (n\text{-}Bu_4N)^+$; (b) $Q^+ = (PPN)^+$; (c) $Q^+ = [\{(C_{18}H_{37})\ 75\% + (C_{16}H_{33})\ 25\%\}_2N(CH_3)_2]^+$. Syntheses are adapted from methods previously described for the preparation of $Q_3[PM_4O_{24}]$,[3a,4–6] using a higher orthophosphoric acid concentration (0.5 equiv/W). Tungstic acid (2.5 g, 10 mmol) was added to 30% hydrogen peroxide (7 mL, 69 mmol). After 40 min of stirring at 60 °C, followed by centrifugation (15 min at 2000 rpm), 6 M H_3PO_4 (0.85 mL, 5.1 mmol) was added to the supernatant liquid. The clear solution (solution A) was stirred for 5 min before isolation of the complex according to one of the following procedures.

(a) Tetrabutylammonium chloride (5.45 g, 20 mmol) dissolved in 10 mL of water was added to solution A. After 5 min of stirring, a white precipitate was filtered off, washed with 10 mL of water and 10 mL of diethyl ether and then air dried (yield: 2.58 g, 67%). Anal. Calcd for $C_{32}H_{73}N_2O_{14}PW_2$: C, 34.67; H, 6.64; N, 2.53; P, 2.79; W, 33.17. Found: C, 35.07; H, 6.82; N 2.60; P, 3.05; W, 33.02. IR (cm^{-1}): 517, 569, 646, 843, 962, 995, 1018. ^{31}P NMR ($MeCN/CDCl_3$; 2 mL/0.5 mL): $\delta = +3.0$ ppm; W satellites $^2J_{PW} = 17$ Hz. ^{183}W NMR ($MeCN/CDCl_3$; 2 mL/0.5 mL): $\delta = -627.3$ ppm; doublet $^2J_{PW} = 17$ Hz.

(b) An aqueous solution of bis(triphenylphosphoranylidene)ammonium chloride (5.75 g, 10 mmol) was slowly added to solution A. After 5 min, the white precipitate was treated as in method a. Anal. Calcd for $C_{72}H_{61}N_2O_{14}P_5W_2$: C, 50.84; H, 3.61; N, 1.65; P, 9.10; W, 21.62. Found: C, 50.96; H, 3.88; N, 1.70; P, 9.05; W, 21.73. ^{31}P NMR ($MeCN/CDCl_3$; 2 mL/0.5 mL): $\delta = +3.2$ ppm.

(c) A solution of Arquad 2HT (3.3 mmol) in 20 mL of $CHCl_3$ was added dropwise to the "$H_2WO_4/H_2O_2–H_2O/H_3PO_4$" system. After 15 min of stirring, the two phases were separated. The organic phase was dried with $MgSO_4$ and the solvent removed using a rotary evaporator. ^{31}P NMR ($CDCl_3$): $\delta = +0.5$ ppm (broad).

Alternative Preparation of 4a from "$H_3[PW_{12}O_{40}]\cdot yH_2O/H_3PO_4/H_2O_2$". $H_3[PW_{12}O_{40}]\cdot yH_2O$ (1.44 g, 0.5 mmol) was dissolved in 2 mL of water. Then 6 M H_3PO_4 (5 mL, 30 mmol) was added. After 5 min of stirring at room temperature, 30% hydrogen peroxide (6 mL, 59 mmol) was added. After 1 h of stirring, an aqueous solution of tetrabutylammonium chloride (10 mmol) was slowly added. After 5 min, a white precipitate was filtered off, washed thoroughly with 10 mL of water and 10 mL of diethyl ether, and then air dried. This product gave spectral and analytical results similar to those obtained for **4a** when it was prepared from "$H_2WO_4/H_2O_2–H_2O/H_3PO_4$" (*vide supra*).

Results

The present study concerns first the analysis of the aqueous phase of the "$H_3[PW_{12}O_{40}]\cdot yH_2O/H_2O_2$" system with excess hydrogen peroxide (e.g. $7 \leq [H_2O_2]/[W] \leq 14$) which is involved in phase transfer catalysis (PTC) for epoxidation of olefins. Typical ^{31}P and ^{183}W NMR spectra are presented in Figures 1 and 2, respectively; the corresponding data (δ and J values) with assignments are given in Tables 3 and 4.

Two synthetic methods afforded the onium salt of (μ-hydrogen phosphato)bis(μ-peroxo)bis(oxoperoxotungstate)(2–).

The synthesis from "H_2WO_4" is based on methods[3,4,6] which generate oxoperoxo species subsequently coordinated by the assembling anion, HPO_4^{2-}. The other procedure involves $H_3[PW_{12}O_{40}]\cdot yH_2O$, which is degraded by excess H_2O_2 to form slightly condensed peroxo species.[4] Addition of orthophosphoric acid leads to the formation of mono-, bi-, tri- and tetranuclear anions; the binuclear species, $[HPW_2O_{14}]^{2-}$, may be precipitated by onium salts such as $n\text{-}Bu_4NCl$ and (PPN)Cl.

The structure of **4a** consists of two formula units of $(n\text{-}Bu_4N)_2[HPW_2O_{14}]$ per unit cell (Table 1). Fractional atomic coordinates are given in Table 2. An ORTEP diagram, Figure 3, shows the structure of the (μ-hydrogen phosphato)bis(μ-peroxo)bis(oxoperoxotungstate)(2–) unit. Selected bond distances and angles are given in Table 5. Additional ^1H NMR study (Figure 4) on a polycrystalline sample was performed to characterize the hydrogen bond between the HPO_4 moities.

Table 3. ^{31}P and ^{183}W NMR Data for the Aqueous $H_3[PW_{12}O_{40}]\cdot yH_2O/H_2O_2$ System ($[H_2O_2]/[W]) = 7$), Corresponding to the Spectra of Figures 1a and 2a

^{31}P			^{183}W			
δ[a]	$^2J_{W-P}$[b,c]	I_{rel}, %	δ[a,d]	$^2J_{W-P}$[b]	I_{rel}, %	assignt
–3.5	25.0 (4W)	15	–667 (d)	25.1	9	$[PW_4O_m]^{\alpha-}$[e]
–1.5	24.4 (3W)	30	–668 (d)	24.1	13	$[PW_3O_n]^{\beta-}$[e]
–0.3	22.9 (2W)	38	–676 (d)	22.8	11	$[PW_2O_p]^{\gamma-}$[e]
+0.3	[f]	17	[g]			$[PWO_q]^{\delta-}$[e]
			–626 (s)		25	[h]
			–698 (s)		42	[h]

[a] δ in ppm relative to H_3PO_4 (^{31}P) and WO_4^{2-} (^{183}W), respectively; negative values correspond to shielding with respect to the reference. [b] J in Hz, ±0.2 Hz. [c] Number of W in parentheses, determined from relative intensity of the tungsten satellites. [d] Multiplicity in parentheses: (d) = doublet; (s) = singlet. [e] This work. [f] Broad resonance satellites not resolved. [g] Not observed. [h] Peroxotungstate species, see ref 15.

Table 4. ^{31}P and ^{183}W NMR Data for the Aqueous $H_3[PW_{12}O_{40}]\cdot yH_2O/H_3PO_4$ System ($[H_2O_2]/[W]/[H_3PO_4] = 7:1:0.75$), Corresponding to the Spectra of Figures 1b and 2b

^{31}P			^{183}W			
δ[a]	$^2J_{W-P}$[b,c]	I_{rel}, %	δ[a,d]	$^2J_{W-P}$[b]	I_{rel}, %	assignt
–3.5		traces				$[PW_4O_m]^{\alpha-}$[e]
–1.5	24.4 (3W)	3	–668 (d)	24.5	8	$[PW_3O_n]^{\beta-}$[e]
–0.3	23.0 (2W)	21	–676 (d)	23.2	38	$[PW_2O_p]^{\gamma-}$[e]
+0.3	22.3 (1W)	50	–675 (d)	22.2	47	$[PWO_q]^{\delta-}$[e]
+0.8		26				free phosphate
			–628 (s)		7	peroxotungstate
			–698 (s)		ε	peroxotungstate[f]

[a–e] See Table 3. [f] See ref 15.

The ^1H MAS NMR spectrum of a polycrystalline sample of $(n\text{-}Bu_4N)_2[HPW_2O_{14}]$ does not allow the static spectrum to be narrowed completely, mainly because of the broadening of the ^1H spectrum by ^{14}N interactions. However, the spectrum contains signals also visible in the MAS + echo spectrum. This spectrum contains poorly resolved signals corresponding to isotropic values of the onium ions and their small spinning side bands, a little more than 7 ppm apart (Figure 4). The characteristic signals are as follows: (i) near 0 ppm, a contribution of R–Me groups; (ii) about 1.8 ppm, that of R–CH_2–R′; (iii) at higher chemical shift values (2–4 ppm), a signal due to resonance of $[R\text{–}CH_2NR'_3]^+$ groups which are broadened by the proximity of ^{14}N. The spectrum also contains a well-defined, relatively narrow signal at 5.4 ppm, which cannot be attributed to the onium ions; it is attributed to the HPO_4 group.

A complementary study was performed by IR (Figure 5) and Raman spectroscopy (Table 6), ^{31}P NMR (analysis of the tungsten satellites subspectra), and ^{183}W NMR (Figure 6) to show that the $[HPW_2O_{14}]^{2-}$ anion is stable in solution and that the overall structure is conserved in aqueous as well as in organic solvents at the early stages of a stoichiometric oxidation reaction.

(*R*)-(+)-Limonene is stoichiometrically epoxidized by **4a**. In the presence of hydrogen peroxide, catalytic systems are generated with a phase transfer agent (Table 7).

Discussion

NMR Characterization of Oxoperoxo Anions, $[PW_xO_y]^{\omega-}$, in the Aqueous Phase (x = 1–4). The ^{31}P NMR spectrum of the "$H_3[PW_{12}O_{40}]\cdot yH_2O/H_2O_2$" system ($[H_2O_2]/[W] \approx 7$) exhibits four peaks with well-resolved tungsten satellites for three of them (Figure 1a). The measured coupling constants are significantly different (Table 3); this allowed us to correlate the ^{31}P signals with the *three ^{183}W NMR doublets* between –660 and –680 ppm (Figure 2a). The most deshielded ^{31}P line (δ = +0.3 ppm) with

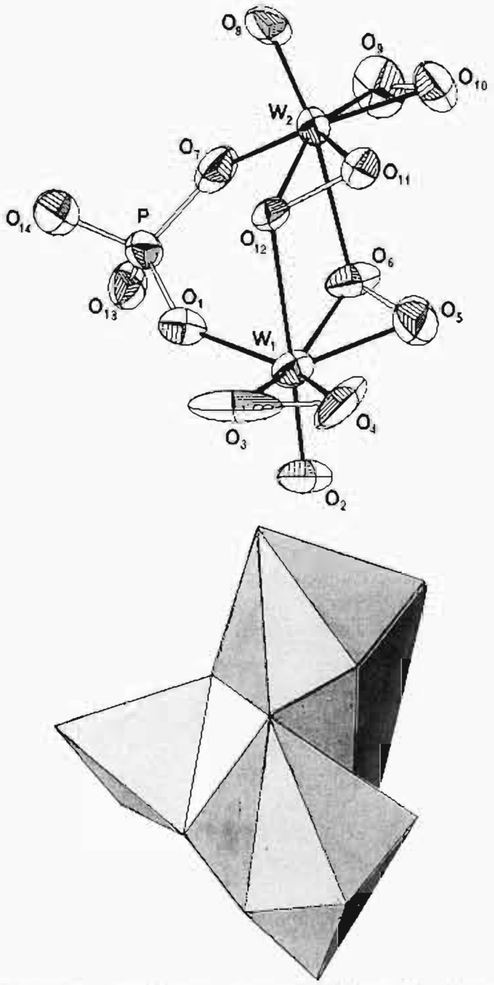

Figure 3. (a) Top: ORTEP view of the $[HPO_4\{WO(\mu\text{-}O_2)(O_2)\}_2]^{2-}$ anion in **4a**, showing the atom-labeling scheme. Atoms are represented by thermal ellipsoids at 50% level. (b) Bottom: Alternative representation of the complex anion.

broad unresolved satellites (two shoulders, Figure 1a), has no evident counterpart in the ^{183}W spectrum (Figure 2a); the corresponding ^{183}W resonance signal is probably relatively broad due to efficient chemical shift anisotropy relaxation.[4b] Addition of H_3PO_4 to this system led to intensity modifications in both the ^{31}P and ^{183}W NMR spectra. Figures 1b and 2b represent typical spectra for $[H_3PO_4]/[W] \approx 0.75$. The ^{183}W lines at −698 ppm, attributed to the $[W_2O_3(O_2)_4(H_2O)_2]^{2-}$ anion,[4b,15] and at −628 ppm, probably due to another oxoperoxotungstate, progressively disappeared with increasing H_3PO_4 concentration. Moreover, a new line at +0.7 ppm, without tungsten satellites, appeared in the ^{31}P spectrum; this line may be assigned to uncoordinated phosphate ion. The intensity variations of other ^{31}P NMR lines, as the H_3PO_4 concentration increased, appeared to be correlated with the intensity of the ^{183}W counterpart but uncorrelated with each other. From these variations, we conclude that the four pairs (^{31}P and associated ^{183}W signals) can be unambiguously assigned *to four different phosphatoperoxotungstate species.*

The relative intensities of the tungsten satellites of the most shielded ^{31}P line ($\delta(^{31}P) = -3.5$ ppm) reveal that the corresponding phosphorus atom is linked to four equivalent W atoms, responsible for the ^{183}W resonance at −667 ppm (doublet, $^2J_{W-P} \approx 25.1$ Hz). Moreover, the relative intensities of the ^{31}P and ^{183}W resonances of this species, with respect to those of the "authentic" trihydrogen phosphododecatungstate, $H_3[PW_{12}O_{40}]\cdot yH_2O$, agree with the stoichiometry P/W = 1/4. The *phosphatoperoxotungstate* then is formulated as $[PW_4O_m]^{\alpha-}$. Following the same procedure, we may assign the −1.5 ppm ^{31}P line and the −668 ppm ^{183}W doublet ($J \approx 24.2_5$ Hz) to a $[PW_3O_n]^{\beta-}$ species. The −0.3 ppm ^{31}P signal and the −676 ppm ^{183}W counterpart ($J \approx 22.8_5$ Hz) correspond to $[PW_2O_p]^{\gamma-}$, while the +0.3 ppm ^{31}P line and the −675 ppm ^{183}W doublet ($J \approx 22.2$ Hz) are related to a $[PWO_q]^{\delta-}$ species. The assignment to "PW_x" species (x = 1–4) is fully consistent with intensity variations observed when the orthophosphoric acid concentration is increased. The phosphorus-rich species (with low W content) increases at the expense of the pure peroxotungsten species. The ^{31}P chemical shift variation is also consistent with the general trend observed for *phosphooxotungstates*: the ^{31}P chemical shift increases as W/P decreases.[16] The "PW_xO_y" complexes can also be generated in separate experiments from the "$H_2WO_4/H_2O_2/H_3PO_4$" systems[17] (see also Experimental Section). These NMR results demonstrate the existence of several equilibria which may be tentatively summarized by

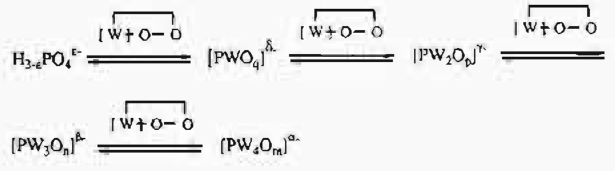

Onium salts were obtained from solutions with high phosphorus concentrations ($[P/W] \approx 0.5-5$); all crystalline samples were found (IR, Raman and NMR) to contain the same "PW_2" anion, but in our hands only the $(n\text{-}Bu_4N)^+$ salt afforded good single crystals corresponding to $(n\text{-}Bu_4N)_2[HPW_2O_{14}]$ (**4a**).

Crystal Structure of 4a. The asymmetric unit consists of a nearly tetrahedral assembling anion, HPO_4^{2-}, and of a neutral moiety, $[W_2O_2(O_2)_4]$, in which the W atoms are seven-coordinated by oxygen atoms in a pentagonal bipyramidal arrangement (*PBPY-7*) (Figure 3). Two oxygen atoms (O(1) and O(7)) of the HPO_4^{2-} anion are corner-sharing with two different basal planes of the pentagonal bipyramid. This results in a slight weakening of the bond between these two oxygen atoms and the tetrahedrally coordinated phosphorus atoms (Table 5), as indicated by the longer P–O bond distances (1.55–1.58 Å) as compared to the 1.48–1.52 Å for the other two P–O bonds involved in hydrogen bonding with another anionic species (*vide infra*). The two W atoms are connected by two μ-peroxo bridges also observed in $[(C_4H_9)_4N]_3[PM_4O_{24}]$ (M = Mo,[5] W[3a]). The two associated pentagonal bipyramids share one edge of the nonbasal plane. The asymmetric dimeric moiety, $[W_2O_2(\mu\text{-}O_2)_2(O_2)_2]$, thus has two distinct pairs of peroxo ligands. To our knowledge, this dimeric unit has not been observed for peroxo tungsten complexes with oxo,[18] oxalate,[19] sulfate,[20] and carbonate[21] as assembling ligands. Similar dimeric units exist only in the $[PW_4O_{24}]^{3-}$ anion.[3a] *Therefore the $[W_2O_2(\mu\text{-}O_2)_2(O_2)_2]$ moiety is a rather unique building block for the two anions*: $[HPW_2O_{14}]^{2-}$ and $[PW_4O_{24}]^{3-}$.

The pentagonal bipyramids of oxygen atoms surrounding the two W atoms are almost identical (see supplementary material). Each girdle (equatorial plane) is generated by two peroxo groups and one oygen atom of the HPO_4^{2-}. One of the apical positions of the girdle axis is occupied by the terminal oxo ligand, O^{2-} (W=O: 1.62–1.71 Å) and the other by a μ-O atom of a bridging peroxo group with a rather long W—O bond (W—O: 2.34 Å). As for the octahedral coordination in polyoxometalates, the W

---

(15) Campbell, N. J.; Dengel, A. C.; Edwards, C. J.; Griffith, W. P. *J. Chem. Soc., Dalton Trans.* **1989**, 1203.

(16) Massart, R.; Contant, R.; Fruchart, J.-M.; Ciabrini, J.-P.; Fournier, M. *Inorg. Chem.* **1977**, *16*, 2916.

(17) (a) Aubry, C. Thesis, Université Pierre et Marie Curie, Paris, 1991. (b) Dengel, A. C.; Griffith, W. P.; Parkin, B. C. *J. Chem. Soc., Dalton Trans.* **1993**, 2683.

(18) Einstein, F. W. B.; Penfold, B. R. *Acta Crystallogr.* **1964**, *17*, 1127.

(19) Hashimoto, M.; Ozeki, T.; Ichida, H.; Sasaki, Y.; Matsumoto, K.; Kudo, T. *Chem. Lett.* **1987**, 1873.

(20) Hashimoto, M.; Iwamoto, T.; Ichida, H.; Sasaki, Y. *Polyhedron* **1991**, *10*, 649.

(21) Stromberg, R. *Acta Chem. Scand., Ser. A* **1985**, *39*, 507.

Table 5. Anion Interatomic Distances (Å) and Bond Angles (deg)

W(1)–O(1)	1.92(2)	W(1)–O(2)	1.62(2)
W(1)–O(3)	1.97(2)	W(1)–O(4)	1.90(2)
W(1)–O(5)	1.86(2)	W(1)–O(6)	1.92(2)
W(1)–O(12)	2.34(2)		
W(2)–O(6)	2.34(1)	W(2)–O(7)	1.94(2)
W(2)–O(8)	1.71(2)	W(2)–O(9)	1.92(2)
W(2)–O(10)	1.66(4)	W(2)–O(11)	1.93(2)
W(2)–O(12)	1.94(2)		
P(1)–O(1)	1.58(2)	P(1)–O(7)	1.55(2)
P(1)–O(13)	1.52(2)	P(1)–O(14)	1.48(2)
O(3)–O(4)	1.53(3)	O(5)–O(6)	1.51(2)
O(9)–O(10)	1.56(4)	O(11)–O(12)	1.47(3)
O(2)–W(1)–O(1)	95.3(9)	O(3)–W(1)–O(1)	88.9(11)
O(3)–W(1)–O(2)	96.6(11)	O(4)–W(1)–O(1)	134.2(10)
O(4)–W(1)–O(2)	99.1(10)	O(4)–W(1)–O(3)	46.5(9)
O(5)–W(1)–O(1)	133.3(9)	O(5)–W(1)–O(2)	105.3(9)
O(5)–W(1)–O(3)	128.4(10)	O(5)–W(1)–O(4)	83.8(9)
O(6)–W(1)–O(1)	86.9(8)	O(6)–W(1)–O(2)	107.8(9)
O(6)–W(1)–O(3)	155.6(9)	O(6)–W(1)–O(4)	128.2(9)
O(6)–W(1)–O(5)	47.1(7)	O(12)–W(1)–O(1)	75.4(7)
O(12)–W(1)–O(2)	169.9(9)	O(12)–W(1)–O(3)	87.1(10)
O(12)–W(1)–O(4)	90.2(9)	O(12)–W(1)–O(5)	79.4(7)
O(12)–W(1)–O(6)	68.6(7)		
O(7)–W(2)–O(6)	73.7(6)	O(8)–W(2)–O(6)	171.7(8)
O(8)–W(2)–O(7)	100.1(8)	O(9)–W(2)–O(6)	86.6(7)
O(9)–W(2)–O(7)	94.7(13)	O(9)–W(2)–O(8)	99.5(9)
O(10)–W(2)–O(6)	94.5(12)	O(10)–W(2)–O(7)	145.1(12)
O(10)–W(2)–O(8)	93.7(12)	O(10)–W(2)–O(9)	51.2(13)
O(11)–W(2)–O(6)	79.8(8)	O(11)–W(2)–O(7)	129.6(10)
O(11)–W(2)–O(8)	100.8(10)	O(11)–W(2)–O(9)	125.9(14)
O(11)–W(2)–O(10)	77.8(14)	O(12)–W(2)–O(6)	68.3(7)
O(12)–W(2)–O(7)	85.4(8)	O(12)–W(2)–O(8)	106.2(9)
O(12)–W(2)–O(9)	153.9(8)	O(12)–W(2)–O(10)	121.2(13)
O(12)–W(2)–O(11)	44.7(9)		
O(7)–P(1)–O(1)	104.3(10)	O(13)–P(1)–O(1)	108.5(11)
O(13)–P(1)–O(7)	109.8(12)	O(14)–P(1)–O(1)	112.5(12)
O(14)–P(1)–O(7)	111.9(11)	O(14)–P(1)–O(13)	109.7(11)
P(1)–O(1)–W(1)	139.3(12)	O(4)–O(3)–W(1)	64.3(11)
O(3)–O(4)–W(1)	69.2(11)	O(6)–O(5)–W(1)	68.5(10)
W(2)–O(6)–W(1)	111.2(8)	O(5)–O(6)–W(1)	64.4(10)
O(5)–O(6)–W(2)	110.3(11)	P(1)–O(7)–W(2)	142.7(12)
O(10)–O(9)–W(2)	55.8(16)	O(9)–O(10)–W(2)	73.0(17)
O(12)–O(11)–W(2)	67.9(13)	W(2)–O(12)–W(1)	110.8(9)
O(11)–O(12)–W(1)	111.2(13)	O(11)–O(12)–W(2)	67.4(12)

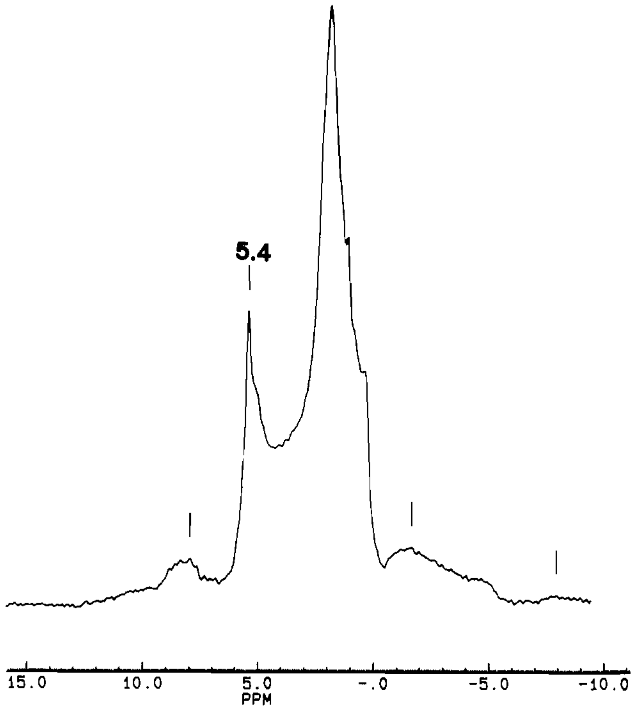

Figure 4. Room-temperature ^1H (MAS + echo method) NMR spectrum of a polycrystalline sample of $(n\text{-}Bu_4N)_2[HPO_4\{WO(\mu\text{-}O_2)(O_2)\}_2]^{2-}$ (**4a**).

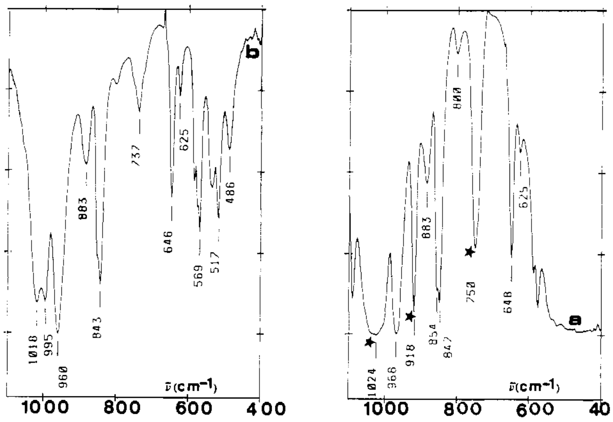

Figure 5. IR spectra: (a) acetonitrile solution of **4a** (0.1 M) in a sodium chloride cell (0.1 mm thick) at room temperature (★: MeCN bands); (b) solid sample of **4a** with Nujol.

atoms are located outside the mean equatorial plane defined by the five equatorial O atoms (0.35 and 0.33 Å for W(1) and W(2), respectively); such distances are also found for other structural units.[18,19,21] One of the non-bridging (or terminal) peroxo groups, O(3)O(4), is symmetrically coordinated to the W atom. W(1)-O(4) and W(1)-O(3) distances are nearly equal and correspond to classical single W–O bonds (1.90–1.97 Å); the O–O distance (1.53 Å) could correspond to a slightly elongated peroxo bond (OWO angle of about 46.5°). The positions of the other non-bridging peroxo groups, O(9) and O(10), are less well-defined; the thermal ellipsoids for these oxygen atoms are too large. This could be due to a significant mean amplitude of vibration for these oxygen atoms. A low-temperature crystal structure determination would perhaps overcome this problem. We shall see (*vide infra*) that there is a good correlation between ν(O–O) and slightly elongated O–O distances.

Hydrogen Bonds between Two Anionic Species. The ^1H NMR signal at 5.4 ppm in the $(n\text{-}Bu_4N)_2[HPW_2O_{14}]$ spectrum (Figure 4) does not correspond to a part of the onium ions; it must be attributed to the $(HPO_4)^{2-}$ groups. The influence of acid strength and hydrogen bond formation on the ^1H isotropic chemical shift (δ) of oxygenated solid acids has been already studied.[22–26] The shift increases with the ionicity of the acid OH bond and with the strength of the hydrogen bonds that may be formed.[23–26] Published results for alkaline monohydrogen phosphates and phosphonic acids of known structures[26] gave higher δ values for the POH group proton than that found here (between 10.3 and 16.2 ppm). This last value is obtained for nitrilotrimethylenetriphosphonic acid with a very short hydrogen bond (2.458 Å for the O···O distance) and for which the acid strength may be increased by the proximity of the organic ligands. However, the 5.4 ppm value of our experiment can be considered as low, especially as the O···O distance of the hydrogen bond between two anionic species in **4a** (Figure 7) is only 2.51 Å. It should be remembered that δ values for inorganic hydrogenosilicates which are not highly polymerized[25] are much greater (12–15 ppm) than those obtained for silanol and even SiOH(Al) acidic groups in H-form zeolites (4–5.5 ppm).[27–28] From our result, we have then to assume the following (i) the ionicity of the OH bond in $(n\text{-}Bu_4N)_2[HPW_2O_{14}]$ is low, which is actually the case for the

---

(22) Berglund, B.; Vaughan, R. W. *J. Chem. Phys.* **1980**, *73*, 2037.
(23) Rosenberger, H.; Grimmer, A.-R. *Z. Anorg. Allg. Chem.* **1979**, *448*, 11.
(24) Schröter, B.; Rosenberger, H.; Hadzi, D. *J. Mol. Struct.* **1983**, *96*, 301.
(25) Heidemann, D.; Grimmer, A.-R. Personal communication.
(26) Harris, R. K.; Jackson, P. *J. Chem. Soc., Faraday Trans. 1* **1988**, *84*, 3649.
(27) Freude, D.; Hunger, M.; Pfeifer, H., *Chem. Phys. Lett.* **1982**, *91*, 307.
(28) Freude, D. *Stud. Surf. Sci. Catal.* **1989**, *52*, 169.

Table 6. Physicochemical Data for the Phosphoperoxometalates

compd	distances,[a] Å						ν(O–O), cm^{-1}			
	M–O$_{\text{peroxo bridging}}$		M–O$_{\text{peroxo}}$		O–O bridging	O–O	IR		Raman	
							solid state	solution	solid state	solution
$Q_3[PMo_4O_{24}]$	1.88	2.00	1.90	1.91	1.48	1.46	868	874	881	883
(**3a**)	1.89	1.98	1.92	1.93	1.48	1.46				
$Q_3[PW_4O_{24}]$	1.95	1.85	1.97	1.88	1.56	1.63	847	849	862	862
(**2**)	1.92	2.03	1.88	1.84	1.43	1.56	854	856		
							883	883		
$Q_2[HPW_2O_{14}]$	1.93	1.94	1.92	1.66	1.51	1.56	843	847	856	859
(**4a**)	1.86	1.92	1.90	1.97	1.47	1.53	852	854		
							883	883		

[a] Distances for **2** from ref 3a; distances for $Q_3[PMo_4O_{24}]$ from ref 5.

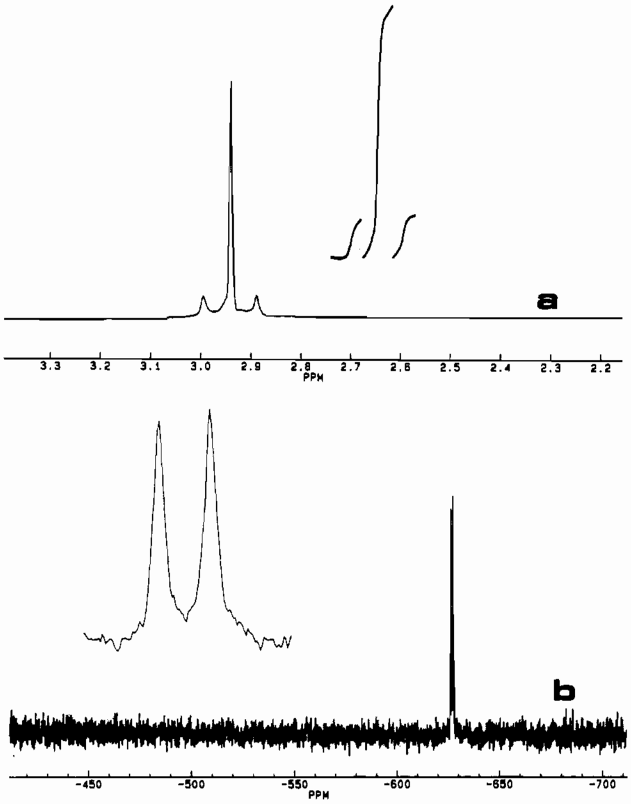

Figure 6. ^{31}P and ^{183}W NMR spectra of a MeCN/CDCl$_3$ (4:1) solution of $(n\text{-}Bu_4N)_2[HPO_4\{WO(\mu\text{-}O_2)(O_2)\}_2]^{2-}$: (a) 162-MHz ^{31}P NMR spectrum (80 scans, without exponential multiplication); (b) 16.6-MHz ^{183}W NMR spectrum (2080 scans, line broadening 1 Hz).

SiOH(Al) groups in zeolites;[29] (ii) the angle of the OH···O hydrogen bond is much less than 180° to be compatible with the known O···O distance.

IR and ^{31}P and ^{183}W NMR Spectra of 4a in Solution. Infrared spectra (ν(O–O) region) suggest that the overall structure of the $[HPO_4\{W(O)(\mu\text{-}O_2)(O_2)\}_2]^{2-}$ anion is maintained in organic solvents (Figure 5a–b). For the acetonitrile solution of the tetrabutylammonium salt, the ^{31}P NMR line ($\Delta\nu_{1/2}$ = 1 Hz) is flanked by well-resolved satellites (Figure 6a) arising from low-abundance isotopomers containing the only magnetically active ^{183}W isotope ($^2J_{W-P}$ = 17.1 Hz).[30] Integration of the satellites with respect to the central line confirms that the phosphorus atom is surrounded by two equivalent tungsten atoms. In addition, the ^{183}W spectrum (Figure 6b) consists of a well-resolved doublet at −627.3 ppm ($\Delta\nu_{1/2}$ = 4.5 Hz; $^2J_{W-P}$ = 17.0 Hz). Both observations are in accordance with the persistence in solution of the $[HPO_4\{W(O)(\mu\text{-}O_2)(O_2)\}_2]^{2-}$ anion with the same overall structure as in the solid state.

Comments on Solvent Effects for δ and J Values. The $[HPO_4\{W(O)(\mu\text{-}O_2)(O_2)\}_2]^{2-}$ anion was first identified and characterized in the aqueous phase by the following NMR parameters (*vide supra*; Tables 1 and 2 and Figures 1 and 2): $\delta(^{31}P)$ = −0.3 ppm; $\delta(^{183}W)$ = −676 ppm, and $^2J_{W-P}$ = 23.1 Hz. After precipitation from this aqueous solution with tetrabutylammonium chloride, the salt may be dissolved in an organic solvent such as acetonitrile. Although the NMR data for the organic solution were always in agreement with the formula, some of them differed markedly from those of the aqueous solution. In particular, the ^{31}P chemical shift became positive ($\delta(^{31}P)$ = +2.95 ppm), the ^{183}W shift was reduced to −627.3 ppm and the tungsten–phosphorus coupling constant was significantly smaller ($^2J_{W-P}$ = 17.05 Hz). The same trend was also observed for the Venturello anion, $[PW_4O_{24}]^{3-}$, for which the ^{31}P and ^{183}W nuclei are deshielded by about 8 ppm (−3.5 to +4.2 ppm) and 74 ppm (−667 to −593 ppm), respectively, and the $^2J_{W-P}$ coupling constant decreases from 25 to 18.5 Hz in the organic solution.[4b] This effect on both *phosphatooxoperoxotungstates* completely overwhelms the so-called solvent effects observed in the polyoxotungstate NMR.[31] Let us remember that the "PW$_2$" and "PW$_4$" anions have no equivalent in oxotungstate chemistry and that such discrete species with both a low degree of condensation and a very low W/P ratio are evidently stabilized by peroxo groups. They remain, however, relatively highly charged, and the external oxygen atoms carry high anionic charge density. Solubilization in organic solvents probably requires ion pairing through specific interactions between the anion and the onium cation, which could induce geometrical and electronic modifications in the oxoperoxoanions and hence explain the observed NMR variations. We propose that the protonation of the $[W_2O_2(\mu\text{-}O_2)_2(O_2)_2]$ moieties could also account for such a difference.

Correlation between O–O Bond Lengths and ν(O–O). We can compare three structures with bidentate peroxo ligands $(n\text{-}Hex_4N)_3[PW_4O_{24}]$,[3a] $(n\text{-}Bu_4N)_2[HPW_2O_{14}]$, and $(n\text{-}Hex_4N)_3[PMo_4O_{24}]$.[5] The M–O$_{\text{peroxo}}$ and O–O bond lengths are given in Table 6. O–O bond distances are significantly greater for the two tungsten complexes. While the O–O distances of the peroxo bond are normally relatively insensitive to the change of ligands,[32] *these results show an effect of the metal.* Moreover, we can correlate these O–O distances with vibrational data (ν(O–O) values from IR and Raman spectroscopy).

Stoichiometric Oxidation Reactions. Catalysis is a wholly kinetic phenomenon, accomplished by intermediates and other transients but not generally by isolable complexes. The ability of **4a** to serve as an effective catalyst precursor led us to compare the resultant high activity with $(n\text{-}Bu_4N)_3[PM_4O_{24}]$ (M = Mo or W). We chose the reaction with (*R*)-(+)-limonene (**5**), which can be performed at 21 °C, the temperature of the physicochemical measurements (Tables 1–6). Figure 8 shows that nearly half the peroxide oxygen is transferred to the olefinic substrate at room

---

[29] Batamack, P.; Dorémieux-Morin, C.; Fraissard J. *J. Chim. Phys.* **1992**, *89*, 423.

[30] Thouvenot, R.; Tézé, A.; Contant, R.; Hervé, G. *Inorg. Chem.* **1988**, *27*, 524.

[31] Gansow, O. A.; Ho, R. K. C.; Klemperer, W. G. *J. Organomet. Chem.* **1980**, *187*, C27.

[32] Jacobson, S. E.; Tang, R.; Mares F. *Inorg. Chem.* **1978**, *17*, 3055.

Table 7. Epoxidation of Limonene by H_2O_2[a]

precursor[b]	[QCl]/[M]	pH_i	pH_f	% conversion	monoepoxides (6a + 6b) yield, %	6a/6b	yield, % diepoxides	yield, % diols
$Q_3[PMo_4O_{24}]$	0.7	1.4	3.5	3	3	0.77	0	0
$Q_3[PW_4O_{24}]$	0.7	1.3	3.5	100	70	4.82	20	10
$Q_2[HPW_2O_{14}]$	0.75	1.4	3.4	90	72	0.97	4	14

[a] General procedure for epoxidation under PTC: $CHCl_3$ (5 mL)/10% H_2O_2 (3 mL; 9.8 mmol); Teflon-coated bar driven externally by a magnetic stirrer; limonene (6.2 mmol); [M]/[limonene] = 2%; phase-transfer agent (QCl) = Arquad 2HT = $\{[(C_{18}H_{37})_2\ (75\%) + (C_{16}H_{33})_2\ (25\%)]N(CH_3)_2\}Cl$; temperature = 21 °C; reaction time = 1 h. pH_i values reported refer to the initial acidity of the aqueous phase in the presence of the organic one. pH_f values reported refer to the acidity at the end of the reaction. [b] See Experimental Section.

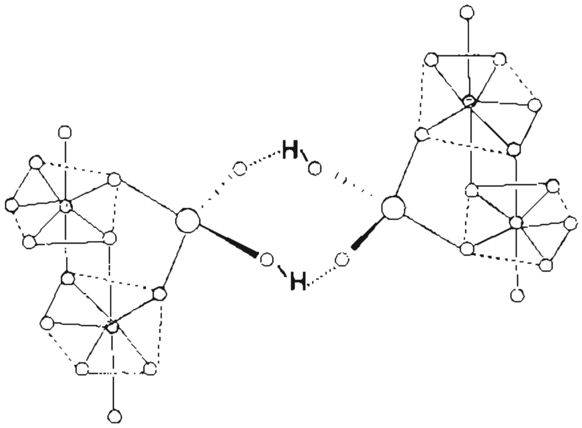

Figure 7. Schematic representation of dimeric anionic species in **4a**.

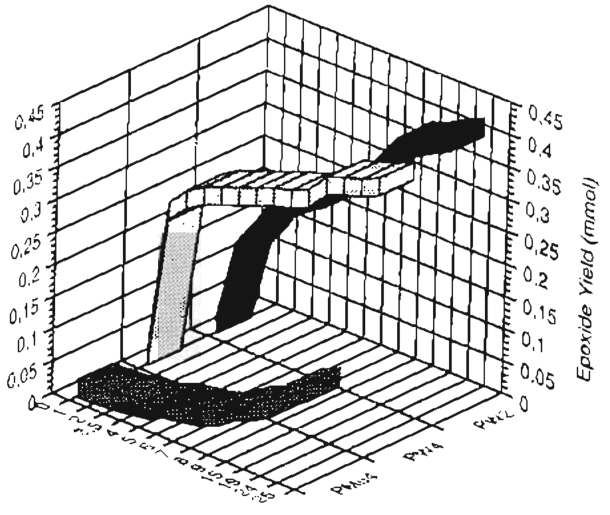

Figure 8. Stoichiometric oxidation reactions under nitrogen using $(n\text{-}Bu_4N)_3[PMo_4O_{24}]$, "$PMo_4$" (0.125 mmol); $(n\text{-}Bu_4N)_3[PW_4O_{24}]$, "$PW_4$" (0.125 mmol); and $(n\text{-}Bu_4N)_2[HPW_2O_{14}]$, "$PW_2$" (0.250 mmol). Epoxide (**6a** + **6b**) formation is plotted versus time; $[O_{peroxo}]$ = 1 mmol; [(*R*)-(+)-limonene] = 1.5 mmol (20 °C and CH_2Cl_2 (5 mL) solvent). Yields are determined by GC using an internal standard.

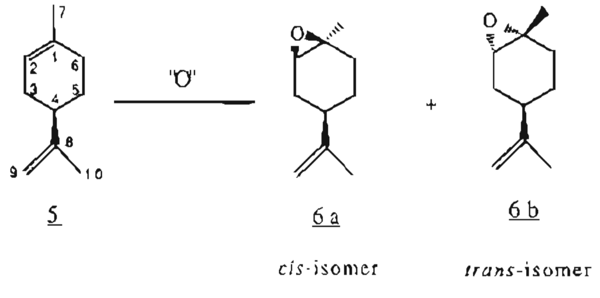

temperature, but only for the tungsten complexes with similar $[W_2O_2(\mu\text{-}O_2)_2(O_2)_2]$ units. This means that only half the peroxo group is available for forming oxygenated products at room temperature. (The primary oxidation products formed are monoepoxides: **6a** and **6b**). A similar observation has been made by Modena's group for a molecular tungsten diperoxo species[33] at 40 °C. The major tungsten (or molybdenum) byproducts in these stoichiometric tests are soluble species which are being studied. In the presence of dilute aqueous solutions of H_2O_2, the active precursor or catalyst can be regenerated, thus forming the basis for catalytic oxidation of alkenes or other substrates by H_2O_2.

Catalytic Tests. The data given in Table 7 (for a biphase medium or PTC) show that the tungsten species are again the most active of the three phosphatooxoperoxo complexes: tungsten(VI) precursors (or catalysts) proved to be 30 times more active than the molybdenum analog. As the overall structure of the anionic peroxo species does not change significantly on going from the solid state to solution, and as in ref 5, we propose to correlate the observed difference between the two tungsten complexes and $Q_3[PMo_4O_{24}]$ with the "O–O bond order" which decreases from the molybdenum complex to the tungsten analog. These results are confirmed with other reactants and will be analyzed more thoroughly elsewhere. In our opinion, the different epoxidation activities of the three complexes which have one bridging and one nonbridging peroxo group on each M(VI) arise from the fact that in the tungsten complexes the O–O bonds are relatively long; this seems to be essential for the facile transfer of the active oxygen. Further work is in progress to isolate other di- or polynuclear species with other assembling ligands.

Conclusion

In the "$H_3[PW_{12}O_{40}]\cdot yH_2O$ or "H_2WO_4"/H_2O_2–H_2O/H_3PO_4" systems with $[H_2O_2]/[W]/[H_3PO_4] \approx 7{:}1{:}0.75$, the spectral data give clear evidence for the formation of *phosphatooxoperoxotungstate species*, $[PW_xO_y]^{q-}$ (x = 1–4). This is confirmed by the isolation of onium salts of the $[PW_xO_y]^{q-}$ anion, but single crystals of good quality were obtained only for $(n\text{-}Bu_4N)_2[HPW_2O_{14}]$, **4a**. The spectral data suggest that the anion of **4a** has the same overall stereochemistry in the solid state and in solution at room temperature. Under the conditions used in our oxidation experiments it appears that the O–O bond order of the oxodiperoxo species is of paramount importance in determining the activation of coordinated peroxide.

Acknowledgment. We thank the CNRS and Chemoxal/L'Air Liquide for a BDI grant to C.A. Thanks are due to Dr. J. S. Lomas for constructive discussions and for correcting the manuscript, to Eurotungstène and Mr. Ph. Lortsch for the gift of tungsten compounds, and to the reviewers for valuable comments. We thank Profs. J.-J. Basselier, J. Fraissard, and J. Livage for NMR facilities. We are grateful to Professor W. P. Griffith for making available a preprint of a related investigation (ref 17b).

Supplementary Material Available: Tables of least-squares planes for the $[HPW_2O_{14}]^{2-}$ anion, the anisotropic thermal parameters for all non-hydrogen atoms, and interatomic distances and bond angles in the cations (3 pages). Ordering information is given on any current masthead page.

---

(33) Amato, G.; Arcoria, A.; Ballistreri, F. P.; Tomaselli, G. A.; Bortolini, O.; Conte, V.; Di Furia, F.; Modena, G.; Valle, G. *J. Mol. Catal.* **1986**, *37*, 165.